

Self-compensation of intrinsic defects in the ternary semiconductor CuGaSe₂

Steffen Schuler, Susanne Siebentritt, Shiro Nishiwaki, Niklas Rega, Joerg Beckmann, Stephan Brehme, and Martha Ch. Lux-Steiner

Hahn-Meitner-Institut Berlin, Glienickerstrasse 100, 14109 Berlin, Germany

(Received 21 October 2002; revised manuscript received 16 April 2003; published 30 January 2004)

Temperature-dependent Hall measurements have been performed on thin films of the ternary chalcopyrite CuGaSe₂. Unintentionally doped samples and Na-containing samples are compared, as well as epitaxial and polycrystalline ones. Acceptor activation energies and acceptor and donor densities are extracted. Activation energies as well as defect densities vary over a wide range. We demonstrate that all samples are dominated by the same defect with an activation energy of 150 meV in the infinite-dilution limit. It is shown that the degree of compensation increases with increasing acceptor density. Thus direct evidence of self-compensation by intrinsic defects is given. CuGaSe₂ containing Na shows the same defects as CuGaSe₂ without Na: thus, it can be excluded that the dominant effect of Na is the introduction of a new acceptor. In addition, reduced compensation due to Na is not found; the net doping increases in spite of an increased compensation.

DOI: 10.1103/PhysRevB.69.045210

PACS number(s): 71.55.-i, 71.22.+i, 72.20.-i

I. INTRODUCTION**A. Self-compensation**

Self-compensation refers to the observation that certain semiconductors “resist” being doped in a certain type or to sufficient doping levels. A review of this phenomenon can be found in the literature.^{1,2} Most of the experimental investigations in this field are concerned with extrinsic doping, and the observation regularly made is that the semiconductor can be either doped only *p* or only *n* type or that the charge carrier concentration does not follow the dopant concentration, but levels off at a certain dopant concentration. The reasons for this effect include the formation of compensating intrinsic defects, either as individual defects or forming a defect pair with the dopant. Others, not involving intrinsic defects, are the amphoteric character of the dopant or insufficient solubility. Very few experimental investigations are available on the effect of self-compensation in intrinsically doped semiconductors. The reason is obvious: it is difficult to control the concentration of doping defects and therefore hard to detect the effect of self-compensation. A number of theoretical papers deal with the effect of self-compensation of and by intrinsic defects. A Fermi-level stabilization model involving amphoteric intrinsic defects was first put forward for GaAs.³ This model was extended to a general doping rule for II-VI and chalcopyrite semiconductors.⁴ The main point is that on an absolute energy scale there are universal stabilization levels below (for *p*-type material) or above (for *n*-type material) which the Fermi level cannot be moved. Thus materials with a high conduction band edge—i.e., low electron affinity—will be much more difficult to dope *n* type since the Fermi level cannot be moved close to the conduction band edge and vice versa for *p*-type materials with a low valence band edge. A microscopic explanation for these universal Fermi energy stabilization levels involves the thermodynamic equilibrium between (intrinsic) defect formation enthalpy and the Fermi level,⁵ thereby giving a mechanism for the effect of the self-compensation.

Ternary materials are prominent among those being intrinsically doped. This includes chalcopyrites, their doping be-

havior being dominated by vacancies, interstitials, or antisites.⁶ They are of practical interest due to their application as absorbers in solar modules^{7,8} and as nonlinear optical materials.^{9,10} Recently, they gained renewed interest as ferromagnetic semiconductors.^{11,12} Their electrical properties are governed by the composition; most of them appear *p* and *n* type depending on the deviation from stoichiometry. CuGaSe₂ ($E_G=1.7$ eV), however, is intrinsically always *p* type. Only in a highly nonequilibrium experiment was it possible to obtain *n*-type CuGaSe₂ by external doping.¹³ To our knowledge there is only one experimental work concerning self-compensation in chalcopyrites: a photoelectron spectroscopy study revealed that upward shifting of the surface Fermi level by surface treatment leads to the loss of Cu from the surface, thus generating Cu vacancies, which are generally considered the main acceptor defects in chalcopyrites.^{14,15} A thermodynamical model involving the electrochemical redox potential of Cu was put forward by the authors explaining the dependence of the defect formation on the Fermi-level position.¹⁴ A detailed *ab initio* calculation of defects in chalcopyrite materials^{16,17} determines the defect formation enthalpy as a function of the Fermi level. For all donor-type defects the formation enthalpy increases with rising Fermi level and for all acceptor-type defects it decreases, thus giving a mechanism for self-compensation.

In this investigation we provide data on the self-compensation of and by intrinsic defects in CuGaSe₂. Due to the use of different preparation methods and substrates, we are able to vary the intrinsic doping over a wide range of concentrations. This includes the use of polycrystalline films deposited onto soda-lime glass as used for solar cell applications. To investigate self-compensation, temperature-dependent Hall measurements are necessary because from these the concentration of acceptors and donors can be extracted. A first temperature-dependent Hall study of polycrystalline chalcopyrites was presented by Kazmerski *et al.*,¹⁸ but was not interpreted in terms of defect concentrations. Since then, no temperature-dependent Hall measurements of polycrystalline chalcopyrites have been published besides our own recent study where we presented mobility

data.¹⁹ The present study presents the first analysis of temperature-dependent Hall measurements of polycrystalline chalcopyrites, concentrating on detailed donor and acceptor data. So far, these measurements have only been available for single crystals and epitaxial films,^{20–22} for polycrystalline material only room-temperature data have been available (see, e.g., Meyer *et al.*²³). Only one study on flash-evaporated CuGaSe₂ thin films also investigated temperature-dependent Hall measurements, but there the focus was on comparison with single crystals, not on defect depths and concentration.²⁴

High concentrations of free carriers have been possible particularly by the use of soda-lime glass among other substrates. It is well known that Na from the glass substrate diffuses into the film at high temperatures during the growth process, thereby increasing the free carrier concentration p .^{25–27} All of these investigations have been performed on CuInSe₂, a chalcopyrite closely related to CuGaSe₂, and its alloy Cu(In,Ga)Se₂ with low Ga content, but the mechanism is believed to be valid for the pure CuGaSe₂ as well. Sodium concentrations of 0.1% in the bulk and of a few percent at the surfaces have been found.^{25,28} Another important observation is the influence of Na on the growth process: grain sizes increase by one order of magnitude when growing under the influence of Na compared to polycrystalline films grown on Na-free substrates.^{25,27,29} Several models for the increased free charge carrier concentration under the influence of Na have been put forward: (a) Na eliminates the donor-type In_{Cu} antisites, thereby reducing the compensation and increasing p (Refs. 30 and 31); (b) Na catalyses the formation of atomic oxygen, thereby allowing the elimination of donorlike Se vacancies by O.^{26,32–34} An acceptorlike substitutional O_{Se} defect was proposed,³³ additionally increasing p : (c) Na forms an acceptorlike substitutional defect Na_{In}, thus increasing p .³⁵ We will show in this contribution that, at least in CuGaSe₂, no hint was found from our detailed study of the temperature-dependent Hall effect and photoluminescence emissions that Na introduces additional defects or decreases the compensation. Nevertheless, the net doping is increased under the influence of Na.

B. Doping in CuGaSe₂

The doping and transport properties of polycrystalline and epitaxial CuGaSe₂ have been investigated before.^{19,36,39} A detailed composition-dependent photoluminescence (PL) study on epitaxial CuGaSe₂ films revealed the existence of two acceptor levels at 60 and 100 meV from the valence band and of a shallow donor, 12 meV below the conduction band.³⁶ They show up in material grown under Cu excess as two donor-acceptor (DA) pair transitions that transform into free-to-bound (FB) transitions at temperatures above 50 K. Ga-rich material shows the same DA transition, but broadened and with a redshift of the peak with increasing Ga content. This behavior is caused by an increasing degree of compensation in these Ga-rich films which causes fluctuating potentials. We find the same PL spectra with the same compositional dependence in polycrystalline films, as well. The assumption of a high degree of compensation is supported by

electrical transport investigations of these epitaxial films by Hall measurements. For epitaxial films grown under varying Cu excess it was demonstrated by temperature-dependent measurements that the mobility around room temperature is always controlled by phonon scattering.³⁷ Films grown under high Cu excess maintain this down to 100 K, whereas films close to stoichiometry show hopping transport at temperatures below 200–250 K. The free charge carrier concentration as a function of temperature of these single-crystalline films was in this former paper³⁷ interpreted in terms of two different acceptor energies at 130 and 80 meV. This was due to the assumption that the thermal defect activation energy has to be constant in all the samples. That this is not the case will be discussed in this contribution. Another investigation turned towards the transport in polycrystalline CuGaSe₂ (Ref. 19): an activated behavior of the mobility was found indicating potential barriers for majority carriers at grain boundaries of about 100 meV height. From the net doping in the films and the barrier height the concentration of charged defects at the grain boundaries was determined to be about 10^{12} cm^{-2} .

In this paper we will present a detailed study of the transport properties of a large variety of different CuGaSe₂ films prepared by different methods (including those discussed in our former papers) with a focus on defect concentrations and compensation.

II. EXPERIMENT

The epitaxial and polycrystalline films in this study are prepared by metal-organic vapor phase epitaxy (MOVPE) and by physical vapor deposition (PVD). Details can be found in Refs. 38 and 39.

By MOVPE epitaxial films are grown on semi-insulating (001) GaAs at substrate temperatures of 570 °C using cyclopentadienyl copper tertiarybutylisocyanide, ditertiarybutyl selenium, and triethyl gallium as the Cu, Se, and Ga source, respectively. The typical thickness of these films is 0.4 μm. The epitaxial quality has been shown by x-ray diffraction (XRD), electron channeling pattern (ECP), and scanning electron microscopy.⁴⁰ Growth rates are low, about 100 nm/h.

The PVD process produces polycrystalline and epitaxial films under the very same preparation conditions. Within one process films can be grown on glass and on semi-insulating (001) GaAs. Soda-lime glass (SLG) and alkali-free (AF) glass AF45 are used. Thermal evaporation from single-elemental sources of Cu, Ga, and Se in a single- or two-stage process at substrate temperatures above 500 °C is used to obtain high-quality films, which are also used as absorbers in solar cells.³⁹ Films grown by PVD are typically 1–1.5 μm thick. Growth rates are high: 2.5 μm/h.

The epitaxial quality of the films obtained from the PVD process is checked by scanning electron microscopy (SEM), XRD, and ECP. XRD shows totally oriented growth in the (001) direction: The only peaks obtained are the (002) and (004) peaks of the substrate and next to them the (004) and (008) reflection of the CuGaSe₂. SEM shows no hint of mosaicking, which can be finally excluded when analyzing

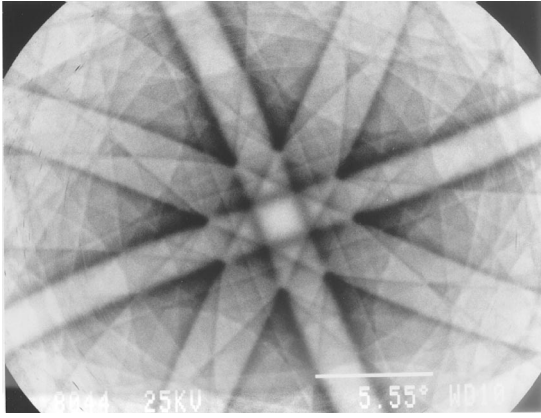


FIG. 1. EC pattern of a CuGaSe_2 film grown by PVD onto (001) GaAs. Epitaxial growth is clearly seen by numerous and crisp lines even out to the edges of the pattern.

the EC pattern in Fig. 1. Epitaxial growth is proved by numerous and crisp lines even out to the edges of the pattern.

To check for residual impurities ERDA (elastic recoil detection analysis) (Refs. 41 and 42) has been performed on epitaxial films from MOVPE and PVD. Both show only an indication of H, C, and O at the surface and interface. Within the film any impurity is below the detection limit of 10 ppm.

All films discussed in this study are grown under Cu excess. This leads to the formation of stoichiometric CuGaSe_2 and a second phase of Cu_{2-x}Se , which segregates to the surface⁴³ and is easily etched away by KCN. All films investigated are etched. From our previous PL study³⁶ it becomes also clear that the defect spectrum of the material grown under Cu excess, although stoichiometric chalcopyrite, depends on the amount of Cu excess during growth. Overall composition is determined by x-ray fluorescence and by energy-dispersive X-ray analysis of the unetched films.

dc Hall measurements are performed at magnetic inductions up to 4 T using a superconducting magnet and van der Pauw geometry with a high-impedance Hall multiplexer setup. For highly resistive samples at low temperatures this enables us to obtain sufficient Hall voltages. Constant-field measurements applying current and field reversal are performed on all samples. Temperature-dependent measurements are carried out in the range from 80 to 350 K. The sample size is $10 \times 10 \text{ mm}^2$, and evaporated Ni/Al contacts show Ohmic behavior at all temperatures. The free carrier concentration p and Hall mobilities μ are calculated from Hall voltages and van der Pauw resistivity measurements using the standard equations $p = r/qR_H$ and $\mu = \sigma/qp$, where R_H is the Hall coefficient, q the elementary charge, and σ the conductivity. For both polycrystalline and epitaxial films the Hall scattering factor r is assumed to be unity since to our knowledge no data or calculations for chalcopyrite materials exist and for polycrystalline materials other uncertainties are probably much greater than any uncertainty in r . This may lead to an underestimation of the carrier concentration and to an overestimation of the mobility. In the case of two-path conduction, as will be discussed later, $1/qR_H$ does not reflect the free carrier concentration anymore, but a superposition of carrier concentrations in the two paths, and

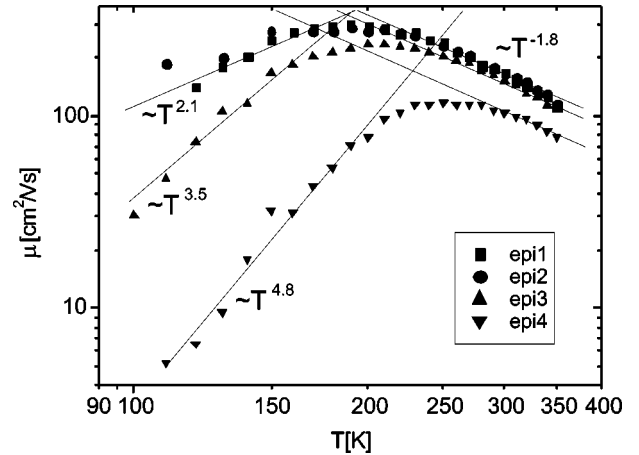


FIG. 2. Temperature dependence of the mobility of several PVD-grown epitaxial films. The steep decrease of the mobility indicates the transition to hopping transport at lower temperatures.

will be labeled the apparent charge carrier concentration. Details of the sample handling and Hall measurements of polycrystalline CuGaSe_2 can be found in Schuler *et al.*¹⁹

III. RESULTS

A. Mobility of PVD-grown epitaxial films

The results on the mobility of MOVPE-grown epitaxial films and of PVD-grown polycrystalline films have been published before^{19,36} and have been discussed in the Introduction.

Figure 2 shows the temperature-dependent mobility $\mu(T)$ of four epitaxial films grown under small amounts of Cu excess and kept in ambient air for different times. The mobility shows a similar behavior in the temperature dependence as has been observed before in MOVPE-grown epitaxial layers with slight Cu excess:³⁷ phonon scattering around room temperature and the transition to hopping conduction at lower temperatures. The lines included in Fig. 2 are the fits to $\mu \sim T^k$. The higher-temperature branch around room temperature follows a $T^{-1.8}$ behavior, which is typical for scattering by acoustical and optical phonons.⁴⁴ At lower temperatures k becomes positive and assumes large values between 2 and 5. Those are much higher than expected for defect scattering and indicate the steep decrease of the mobility with decreasing temperature that is typical for the transition to hopping conduction.^{45,46} The temperature of the mobility maximum can be considered as the onset temperature, below which the influence of hopping will show. The steepness of the mobility decrease increases with the onset temperature. This is not surprising since with increasing defect density one expects the influence of hopping up to higher temperatures and a stronger influence of hopping as seen by the steeper mobility decay. As a tendency, we observe the higher onset temperature with longer exposition times to ambient atmosphere. This is the only difference from MOVPE epitaxial CuGaSe_2 films: in those films no change in ambient atmosphere is observed. The onset temperature observed in the temperature dependence of the mobility correlates

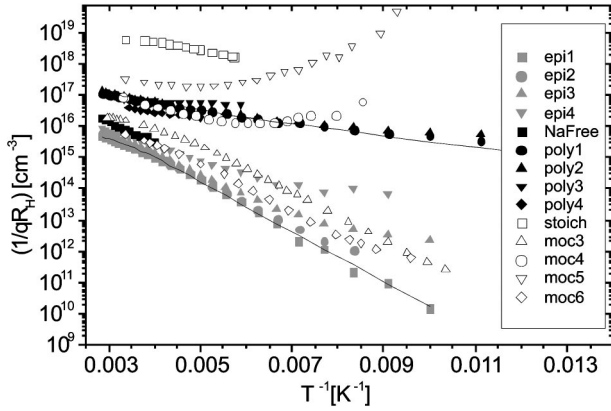


FIG. 3. Temperature dependence of a number of PVD-grown epitaxial and polycrystalline and MOVPE-grown epitaxial samples. Polycrystalline films are grown on Na containing and Na free glass. Clearly seen is that a higher carrier concentration is associated with a lower activation energy.

with the temperature at which hopping starts to influence the apparent charge carrier concentration, as will be shown in the next paragraphs.

It is interesting to see that the temperature-dependent mobility of polycrystalline films also shows a transition just below 200 K from band transport to hopping transport. There the transition shows up as a change in the mobility activation energy (see Ref. 19 for a detailed discussion).

B. Charge carrier concentration

The temperature dependence of the charge carrier concentration $1/qR_H(T)$ for a number of polycrystalline and epitaxial films is shown in Fig. 3. The charge carrier concentration determined in the polycrystalline films is interpreted as the carrier concentration in the bulk of the grains, since the depletion zone along the grain boundaries is small compared to the grain size.^{19,47} Three different types of curves can be distinguished: (1) those following an exponential freeze-out behavior down to the lowest measurement temperatures, (2) those with a small deviation from freeze-out behavior with somewhat higher apparent carrier concentration, but still monotonically falling with decreasing temperature, and (3) those with a minimum in the apparent carrier concentration followed by an increased concentration towards lower temperatures.

The latter is exactly the behavior that is expected for a transport mechanism with two paths, band transport and defect (hopping) transport, having different temperature dependences. In such a two-path system the Hall coefficient R_H is given by⁴⁸

$$R_H = \frac{(p\mu + p_D\mu_D^2)}{q(p\mu + p_D\mu_D)^2}, \quad (1)$$

where p and μ denote the free carrier concentration and mobility in the valence band and p_D and μ_D the concentration and hopping mobility of holes in defects: q is the elementary charge. The Hall factor r is assumed to equal 1 in Eq. (1).

The total number of available charge carriers equals the net doping P , which results from the difference in acceptor N_A and donor N_D concentrations:

$$p + p_D = P = N_A - N_D. \quad (2)$$

At high temperatures all defects are ionized and $p \approx P$; thus, Eq. (1) is dominated by p , whereas p_D can be neglected, resulting in the well-known relationship for single-path transport. At low temperatures, on the other hand, all carriers are located in the defects—i.e., $p_D \approx P$ —and p can be neglected. Therefore at high and low temperatures R_H equals $1/qP$, with a maximum of R_H —i.e., a minimum of the apparent carrier density in between. Samples with type-(3) temperature-dependent carrier concentration show the minimum, while type-(2) samples only start to show the influence of hopping conduction; the minimum would occur at lower temperatures.

Finally, type-(1) samples do not show any significant influence of hopping within the measured temperature range. The difference is due to the defect density, as will be shown later: higher defect density means higher μ_D and thus a more significant influence of hopping. In the following only the high-temperature part where the charge carrier concentration is dominated by band transport is considered since this transport mechanism allows the determination of defect activation energies and concentrations.

A clear tendency is already seen without fitting the data: with higher free carrier concentration the slope is shallower—i.e., the acceptor activation energy is smaller. Moreover, polycrystalline films grown on SLG show all a rather high net doping, while the film grown on AF glass (sample labeled “Na free”) shows a considerably lower doping level.

To extract detailed data on defect concentration and defect depths we use the charge-neutrality equation (2), the Fermi distribution for the density of acceptors occupied by holes:

$$p_D = N_A \left(\frac{1}{1 + g \exp\left(\frac{E_F - E_a}{kT}\right)} \right), \quad (3)$$

where E_F is the Fermi energy, E_a the acceptor energy position, k the Boltzmann constant, g the degeneracy factor $= \frac{1}{2}$, and the Boltzmann approximation for the density of free holes in the valence band:

$$p = N_V \exp\left(-\frac{E_F - E_V}{kT}\right), \quad (4)$$

where N_V describes the effective density of states in the valence band and is calculated assuming a relative effective hole mass of 1, and E_V describes the energy position of the valence band edge. Equations (2)–(4) together result in a quadratic equation⁴⁴ which can be solved for p :

$$p = -A + \sqrt{A^2 + gN_V(N_A - N_D)\exp(-E_a/kT)}, \quad (5)$$

with

TABLE I. Acceptor N_A and donor N_D concentrations, net doping P , acceptor activation energy E_A , and degree of compensation, K , of samples prepared by PVD (epix, polyx, Na-free) and MPVPE (mocx).

Sample	N_A (cm ⁻³)	N_D (cm ⁻³)	P (cm ⁻³)	E_A (meV)	K
epi1	8.05×10^{16}	7.37×10^{16}	6.8×10^{15}	141	0.92
epi2	2.22×10^{17}	2.12×10^{17}	1.0×10^{16}	128	0.96
epi3	5.51×10^{17}	5.35×10^{17}	1.6×10^{16}	112	0.97
epi4	1.71×10^{18}	1.69×10^{18}	2.0×10^{16}	83	0.99
Na-free	7.28×10^{18}	7.11×10^{18}	1.7×10^{17}	91	0.98
poly1	1.88×10^{19}	1.84×10^{19}	3.5×10^{17}	26	0.98
poly2	1.96×10^{19}	1.91×10^{19}	4.9×10^{17}	26	0.98
poly3	2.07×10^{19}	2.03×10^{19}	3.8×10^{17}	20	0.98
poly4	1.06×10^{19}	1.04×10^{19}	2.0×10^{17}	32	0.98
poly5	2.48×10^{19}	2.43×10^{19}	4.5×10^{17}	13	0.98
poly6	4.17×10^{19}	4.13×10^{19}	3.9×10^{17}	18	0.99
moc1	1.40×10^{17}	1.21×10^{17}	1.9×10^{16}	116	0.86
moc2	1.96×10^{19}	1.91×10^{19}	4.2×10^{17}	29	0.98
moc3	4.07×10^{16}	1.73×10^{16}	2.3×10^{16}	137	0.43
moc4	1.28×10^{19}	1.23×10^{19}	5.6×10^{17}	46	0.96
moc5	3.93×10^{19}	3.71×10^{19}	2.1×10^{18}	14	0.95
moc6	7.90×10^{16}	6.94×10^{16}	9.7×10^{15}	125	0.88
moc7	7.21×10^{16}	4.98×10^{16}	2.2×10^{16}	130	0.69
moc8	1.68×10^{17}	1.49×10^{17}	1.9×10^{16}	113	0.89
moc9	1.12×10^{18}	1.07×10^{18}	5.0×10^{16}	83	0.96
moc10	4.72×10^{17}	4.41×10^{17}	3.1×10^{16}	117	0.93
moc11	7.26×10^{16}	2.41×10^{16}	4.9×10^{16}	140	0.33

$$A = \frac{1}{2} [N_D + gN_V \exp(-E_A/kT)],$$

where $E_A = E_a - E_V$ is the acceptor activation energy. Equation (5) is used to fit the data in Fig. 3, which are shown for selected samples only, for better visibility. The data are fitted in the whole temperature range for type-(1) samples. Type-(2) and -(3) samples are fitted in the high-temperature region where no deviation from the Arrhenius-like freeze-out behavior occurs. The appearance of high defect concentrations combined with an extreme degree of compensations leads to an uncertainty in deriving the exhaustion value of $p(T)$, which equals $P = (N_A - N_D)$. However, the fits result in values covering some orders of magnitudes, making these uncertainties negligible with respect to the deduced conclusions. The results of the fit are summarized in Table I. A large variation of defect concentrations between 10^{16} and 10^{19} cm⁻³ is covered, resulting also in a large range of degree of compensation, $K = N_D/N_A$, from 33% to 99%. This comes along with a large variation of acceptor activation energies from 10 to 140 meV. The sample labeled “stoich” is different from the other ones in that it was grown under negligible Cu excess and its over all composition is very close to stoichiometry. It shows a very high carrier concentration of 10^{19} cm⁻³ at 300 K, which hints at degeneration. Therefore this sample is excluded from the analysis. It can also be seen from Table I and Fig. 3 that the samples with the highest acceptor concentrations are those that show a minimum in the apparent charge carrier density dependent on temperature.

To clarify the question whether the appearance of different acceptor activation energies is related to the existence of various defects, the defect spectra are studied under optical excitation by photoluminescence measurements. An epitaxial sample with a thermal defect activation energy of 141 meV (epi1) and a polycrystalline sample grown on soda-lime glass with an activation energy of 26 meV (poly1) are compared in Fig. 4. Part (a) shows the as-measured spectra. Both spectra show as the main peak the well-known DA emission at about 1.62 eV (Ref. 36) together with three phonon replica at energies differences of 33 meV, the energy of the LO phonon, as expected for samples grown under moderate Cu excess. Both spectra show also well-resolved exciton emissions (EX). They differ somewhat in energy with the exciton energy of the polycrystalline sample slightly higher by 7 meV; this is due to a higher amount of strain in the epitaxial sample.³⁶ The epitaxial sample shows, in addition to CuGaSe₂ emission, near-band-edge emission from the GaAs substrate. The intensity of the polycrystalline sample is about one order of magnitude higher than that of the epitaxial sample. This is related to the higher defect density found in the polycrystalline sample (see Table I), provided that the defects observed in the Hall experiment are optically active. For better comparison, part (b) shows the spectra normalized in intensity and shifted in energy; i.e., the spectrum of the polycrystalline sample is shifted down by 7 meV to have the two excitonic emissions at the same energy position. As can be seen from Fig. 4(b), besides some broadening of the spectrum of the polycrystalline sample the two normalized spectra seem to be identical. This indicates that the defects which

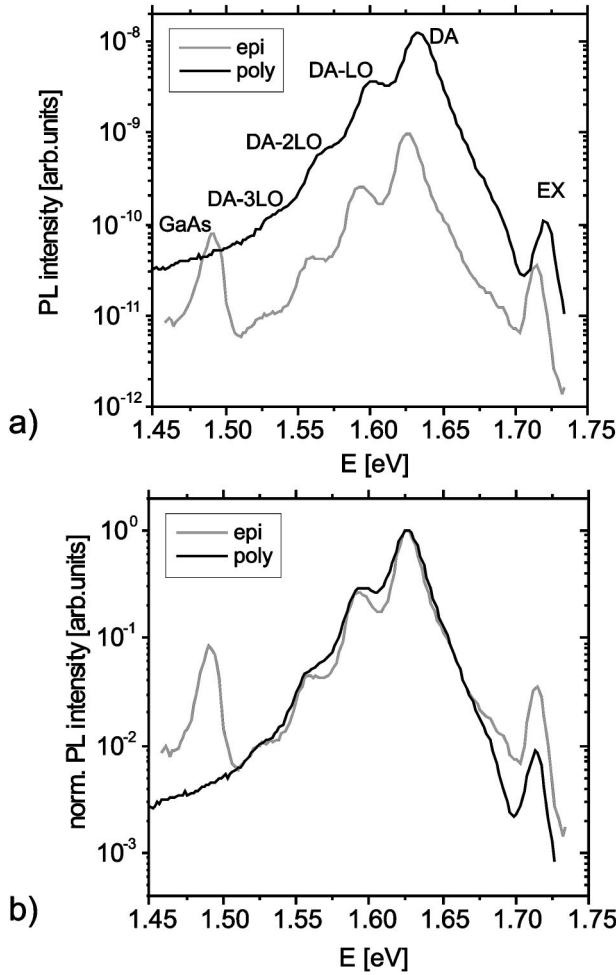


FIG. 4. Photoluminescence spectra ($T=10$ K, $\lambda=514.5$ nm) of an epitaxial and a polycrystalline sample with high and low thermal activation energies. (a) As-measured spectra and (b) spectra normalized in intensity and shifted in energy. Visible is the excitonic emission (EX), a donor-acceptor-pair transition (DA), and its phonon replica (DA-LO) and emission from the GaAs substrate (GaAs). Note the logarithmic scale of the intensity.

are involved in the light emission process in the sample with the high acceptor activation energy and the sample with the low acceptor activation energy are identical.

IV. DISCUSSION

We would like to discuss first the different acceptor activation energies and subsequently the observed defect concentrations showing the effect of self-compensation.

It was observed in 1949 by Pearson and Bardeen that the thermal defect activation energy, as determined by analysis of Hall measurements, depends on the defect concentration—namely, linearly on the third root of the density.⁴⁹ Later, it was shown that the effect occurs pronouncedly in compensated semiconductors and the linear dependence on the third root is not on the concentration of the defect itself, but on the concentration of the compensating defects.⁵⁰ Several models from screening by free electrons⁴⁹ to overlapping defect levels, band tailing, and fluctuating potentials⁵¹ have

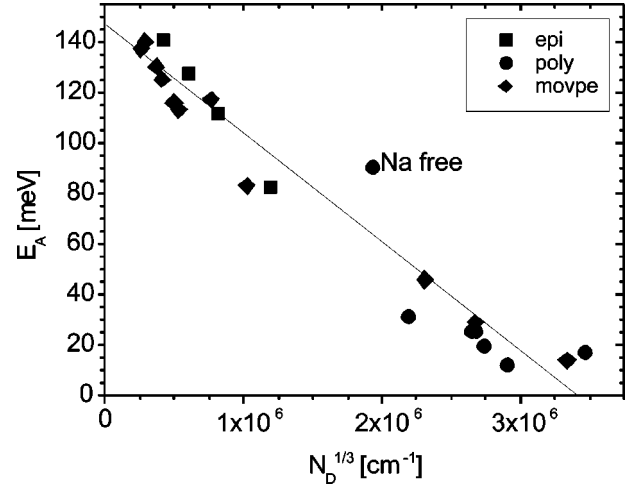


FIG. 5. Activation energy vs third root of donor concentration results in a linear relation.

been put forward, but to our knowledge no conclusive model has been reached up to date. The optical ionization energy of a defect is not known to vary with the defect density⁵⁰ (which complies with the observation of identical PL spectra in Fig. 4). Nevertheless, it has been observed in a wide range of semiconductor materials^{50,52} that the thermal defect activation energy E_A depends on the density N_D :

$$E_A = E_0 - \alpha N_D^{1/3}, \quad (6)$$

with the infinite dilution limit E_0 and a slope α typically around 4×10^{-8} eV cm.

In Fig. 5 the acceptor activation energies of the samples in Fig. 3 and Table I are plotted versus the third root of the compensating donor density. A linear dependence with a slope α of $(4.3 \pm 0.3) \times 10^{-8}$ eV cm and an infinite dilution limit of the activation energy of 147 ± 5 meV is found. This together with the photoluminescence results confirms the assumption that all samples show the same acceptor defect with an activation energy around 150 meV in the infinite-dilution limit.

The fact that acceptor and donor densities exceed 10^{19} cm⁻³ should imply the presence of strong potential fluctuations caused by their statistical distribution,⁴⁸ resulting in the absence of sharp DA recombination peaks. However, it is known from chalcopyrites that the formation of defect complexes—i.e., spatially correlated defects—is possible.¹⁶ Thus strong potential fluctuations need not be expected even at high defect densities if donors and acceptors are not statistically distributed, but are correlated in pairs or clusters. In Fig. 6 we show the PL spectra of the stoichiometric sample “stoich” with charge carrier concentrations as high as 10^{19} cm⁻³. This implies even higher defect concentrations for this sample. The spectra is characterized by sharp DA peaks, contradicting the presence of strong potential fluctuations caused by statistically distributed defects. As a consequence, we propose the existence of spatially correlated defect complexes. Differently from the PL spectra of Cu-rich samples as in Fig. 4 where the DA emission is correlated to a 100-meV acceptor,³⁶ the stoichiometric sample is charac-

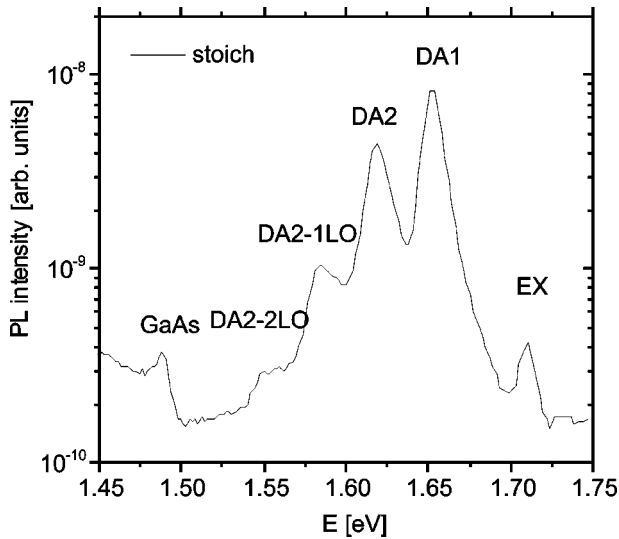


FIG. 6. PL spectra of the sample “stoich” with high defect density and sharp DA emission peaks.

terized by two DA emissions originating from two acceptors at 60 and 100 meV.³⁶ At this point of research we are not able to relate the two different acceptors, found in PL studies, to the acceptor at 150 meV in the infinite-dilution limit, as determined by Hall experiments. Further experiments using other methods of defect spectroscopy must be conducted to clarify this matter.

Despite these open questions, we now focus on the defect densities of the studied samples. Covering more than 3 orders of magnitude, as seen in Table I, this allows the study of compensational effects over a wide concentration range. In Fig. 7(a) we plot the degree of compensation for all samples investigated versus the acceptor density. It becomes clear that with increasing acceptor density the degree of compensation also increases. When a certain acceptor concentration is reached, the samples are almost completely compensated and seem to resist a further intrinsic p doping by generating donors spontaneously. Two requirements are fulfilled for a theoretical explanation of this phenomena: low or even negative defect formation enthalpies and their dependence on the Fermi level.¹⁶ When including more acceptors in the material the Fermi level would shift down. This in turn decreases the enthalpy of formation for the donor defects¹⁶ and thus more donors are formed, increasing the compensation. Self-compensation is evident. Nevertheless, the net doping is increased with increasing acceptor concentration as seen from Fig. 7(b). When concentrating on the polycrystalline samples it is evident that the samples prepared on sodium-containing glass show in fact higher net doping, as was observed before. But this is not due to a decreased compensation as is generally believed (see the Introduction). On the contrary the net doping increases in spite of an increasing compensation. From Figs. 4 and 5 it was concluded that all samples show the same defect. The Na-containing samples show no additional transition in PL and fit very well into the dependence of E_A on $N_D^{1/3}$ defined by the epitaxial (Na-free) samples. There is no hint at an additional acceptor defect

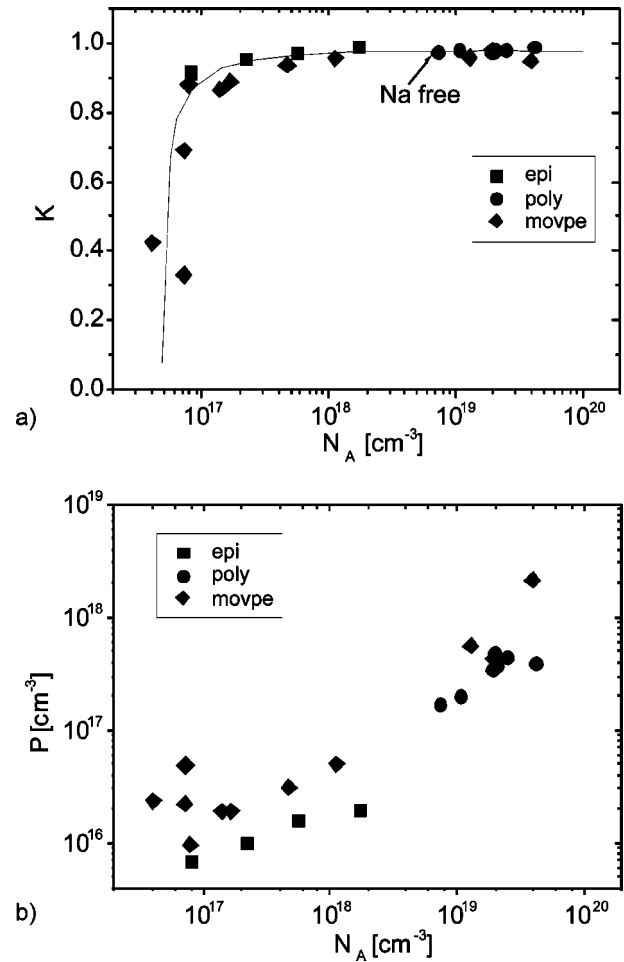


FIG. 7. Degree of compensation (a) and net doping (b) as a function of acceptor density.

generated by Na. In fact, it is evident that Na increases the density of intrinsic acceptor defects, but does not create a new type of defect.

V. SUMMARY AND CONCLUSION

Hall measurements have been performed on the ternary chalcopyrite CuGaSe_2 .

Unintentionally doped samples and Na-containing samples are compared, as well as epitaxial and polycrystalline ones. The free carrier concentration and mobility as a function of temperature indicate hopping conduction at a temperature below approximately 250–200 K. The free carrier concentration in the temperature range dominated by band transport is fitted by the standard semiconductor statistics equations; acceptor activation energies and acceptor and donor densities are extracted. Acceptor activation energies vary over a wide range. This is due to the wide range of donor densities investigated and the often-established dependence of the majority defect activation energy on the minority defect concentration. In addition, the photoluminescence spectra of samples with very different acceptor activation energies and defect concentrations can basically be identical. Concerning the transport properties, it could be shown that

all samples are dominated by the same defect with an infinite-dilution limit of 150 meV. It is shown that the degree of compensation increases with increasing acceptor density. Thus direct evidence of self-compensation by intrinsic defects is given. We propose that the existence of spatially correlated defect complexes plays an important role in the defect chemistry of CuGaSe₂. The nature of the DA recombination will be further studied by, e.g., time-dependent PL measurements to check this conclusion. CuGaSe₂ containing Na shows the same defect as CuGaSe₂ without Na; thus, it can be excluded that the dominant effect of Na is the introduction of a new acceptor. It has been argued previously that

the increased net doping observed in Na containing chalcopyrites is due to a reduced degree of compensation. Our investigation shows that the contrary is the case: the net doping increases in spite of an increased compensation.

ACKNOWLEDGMENTS

The authors gratefully acknowledge numerous discussions with Rolf Rentsch and Alexander Meeder. We would like to thank Franz Haug and Peter Wägli for the ECP measurements.

- ¹N. V. Agrinskaya and T. V. Mashovets, *Semiconductors* **28**, 843 (1994).
- ²U. V. Desnica, *Prog. Cryst. Growth Charact. Mater.* **36** (4), 291 (1998).
- ³W. Walukiewicz, *J. Vac. Sci. Technol. B* **6**, 1257 (1988).
- ⁴S. B. Zhang, S.-H. Wei, and A. Zunger, *J. Appl. Phys.* **83**, 3192 (1998).
- ⁵S. B. Zhang, S.-H. Wei, and A. Zunger, *Phys. Rev. Lett.* **84**, 1232 (2000).
- ⁶C. Rincon and S. M. Wasim, in *Proceedings of the 7th International Conference Ternary and Multinary Compounds*, edited by S. K. Deb and A. Zunger (Materials Research Society, Pittsburgh, 1987), p. 443.
- ⁷U. Rau and H. W. Schock, *Appl. Phys. A: Mater. Sci. Process.* **69**, 131 (1999).
- ⁸S. Siebentritt, *Thin Solid Films* **403-404**, 1 (2002).
- ⁹S. N. Rashkeev and W. R. L. Lambrecht, *Phys. Rev. B* **63**, 165212 (2001).
- ¹⁰C. O. Ohmer and R. Pandey, *MRS Bull.* **23**, 16 (1998) and other articles in this review issue.
- ¹¹G. A. Medvedkin, T. Ishibashi, T. Nishi, K. Hayata, Y. Hasegawa, and K. Sato, *Jpn. J. Appl. Phys., Part 2* **39**, L949 (2000).
- ¹²S. Cho, S. Choi, G. Cha, S. C. Hong, Y. Kim, Y. Zhao, A. J. Freeman, J. B. Ketterson, B. J. Kim, Y. C. Kim, and B. Choi, *Phys. Rev. Lett.* **88**, 257203 (2002).
- ¹³J. H. Schön, J. Oestreich, O. Schenker, H. Riazhi-Nejad, M. Klenk, N. Fabre, E. Arushanov, and E. Bucher, *Appl. Phys. Lett.* **75**, 2969 (1999).
- ¹⁴A. Klein, J. Fritsche, W. Jaegermann, J. H. Schön, C. Kloc, and E. Bucher, *Appl. Surf. Sci.* **166**, 508 (2000).
- ¹⁵A. Klein and W. Jaegermann, *Appl. Phys. Lett.* **74**, 2283 (1999).
- ¹⁶S. B. Zhang, S.-H. Wei, and A. Zunger, *Phys. Rev. B* **57**, 9642 (1998).
- ¹⁷A. Zunger, S. B. Zhang, and S.-H. Wei, in *Proceedings of the 26th IEEE PV Specialist Conference*, edited by P. Basore (AIP, Woodbury, NY, 1997), p. 313.
- ¹⁸L. L. Kazmerski, M. S. Ayyagari, and G. A. Sanborn, *J. Appl. Phys.* **46**, 4865 (1975).
- ¹⁹S. Schuler, S. Nishiwaki, J. Beckmann, N. Rega, S. Brehme, S. Siebentritt, and M. C. Lux-Steiner, in *Proceedings of the 29th IEEE Photovoltaic Specialist Conference* (IEEE, New York, 2002), p. 504.
- ²⁰B. Schumann, A. Tempel, G. Kühn, H. Neumann, N. V. Nam, and T. Hänsel, *Krist. Tech.* **13**, 1285 (1978).
- ²¹L. Mandel, R. D. Tomlinson, M. J. Hampshire, and H. Neumann, *Solid State Commun.* **32**, 201 (1979).
- ²²D. J. Schroeder, J. L. Hernandez, G. D. Berry, and A. A. Rockett, *J. Appl. Phys.* **83**, 1519 (1998).
- ²³T. Meyer, F. Engelhardt, J. Parisi, and U. Rau, *J. Appl. Phys.* **91**, 5093 (2002).
- ²⁴M. Rusu, P. Gashin, and A. Simashkevich, *Sol. Energy Mater. Sol. Cells* **70**, 175 (2001).
- ²⁵M. Bodegard, L. Stolt, and J. Hedström, in *Proceedings of the 14th European Photovoltaic Solar Energy Conference*, edited by R. Hill, W. Palz, and P. Helm (H. S. Stephens & Assoc., Bedford, 1994), p. 1743.
- ²⁶M. Ruckh, D. Schmid, M. Kaiser, R. Schäffler, T. Walter, and H. W. Schock, in *Proceedings of the First World Conference on Photovoltaic Energy Conversion* (IEEE, New York, 1994), p. 156.
- ²⁷V. Probst, J. Rimmasch, W. Riedl, W. Stettner, J. Holz, H. Harms, and F. Karg, in *Proceedings of the First World Conference on Photovoltaic Energy Conversion* (Ref. 26), p. 144.
- ²⁸D. W. Niles, M. Al-Jassim, and K. Ramanathan, *J. Vac. Sci. Technol. A* **17**, 291 (1999).
- ²⁹V. Probst, F. Karg, J. Rimmasch, W. Riedl, W. Stettner, H. Harms, and O. Eibl, in *Thin Films for Photovoltaic and Related Device Applications*, edited by D. Ginley, A. Catalano, H. W. Schock, C. Eberspacher, T. M. Peterson, and T. Wada, *MRS Symposia Proceedings No. 426* (Materials Research Society, Pittsburgh, 1996), p. 165.
- ³⁰M. A. Contreras, B. Egaas, P. Dippo, J. Webb, J. Granata, K. Ramanathan, S. Asher, A. Swartzlander, and R. Noufi, in *Proceedings of the 26th IEEE Photovoltaic Specialist Conference* (IEEE, New York, 1997), p. 359.
- ³¹S.-H. Wei, S. B. Zhang, and A. Zunger, *J. Appl. Phys.* **85**, 7214 (1999).
- ³²M. Ruckh, D. Schmidt, M. Kaiser, R. Schäffler, T. Walter, and H. W. Schock, *Sol. Energy Mater. Sol. Cells* **41/42**, 335 (1996).
- ³³L. Kronik, D. Cahen, and H. W. Schock, *Adv. Mater. (Weinheim, Ger.)* **10**, 31 (1998).
- ³⁴L. Kronik, D. Cahen, U. Rau, R. Herberholz, H. W. Schock, and J.-F. Guillemoles, in *Proceedings of the 2nd World Conference on Photovoltaic Solar Energy Conversion*, edited by J. Schmidt, H. A. Ossenbrinck, P. Helm, H. Ehmman, and E. D. Dunlop

- (Joint Research Center European Commission, Ispra, 1998), p. 453.
- ³⁵D. W. Niles, K. Ramanathan, F. Hasoon, R. Noufi, B. J. Tielsch, and J. E. Fulghum, *J. Vac. Sci. Technol. A* **15**, 3044 (1997).
- ³⁶A. Bauknecht, S. Siebentritt, J. Albert, and M. C. Lux-Steiner, *J. Appl. Phys.* **89**, 4391 (2001).
- ³⁷S. Siebentritt, A. Gerhard, S. Brehme, and M. Lux-Steiner, in *II-VI Compound Semiconductor Photovoltaic Materials*, edited by R. Birkmire, R. Noufi, D. Lincot, and H.-W. Schock, MRS Symposia Proceedings No. 668 (Materials Research Society, Pittsburgh, 2001), p. H.4.4.1.
- ³⁸M. C. Artaud-Gillet, S. Duchemin, R. Odedra, G. Orsal, N. Rega, S. Rushworth, and S. Siebentritt, *J. Cryst. Growth* **248**, 163 (2003).
- ³⁹S. Schuler, S. Nishwaki, M. Dziedzina, R. Klenk, S. Siebentritt, and M. C. Lux-Steiner, in *II-VI Compound Semiconductor Photovoltaic Materials*, edited by R. Birkmire, R. Noufi, D. Lincot, and H.-W. Schock, MRS Symposia Proceedings No. 668 (Materials Research Society, Pittsburgh, 2001), p. H5.14.1.
- ⁴⁰A. Bauknecht, U. Blieske, T. Kampschulte, A. Ennaoui, V. Nadeuau, H. W. Schock, A. N. Tiwari, M. Krejci, S. Duchemin, M.-C. Artaud, L. M. Smith, S. Rushworth, J. Söllner, and M. C. Lux-Steiner, in *Proceedings of the 2nd World Conference and Exhibition on Photovoltaic Solar Energy Conversion*, edited by J. Schmid, H. A. Ossenbrink, P. Helm, H. Ehmann, and E. D. Dunlop (Joint Research Center European Commission, Ispra, 1998), p. 2436.
- ⁴¹J. C. Barbour, B. L. Doyle, G. W. Arnold, J. E. E. Baglin, P. F. Green, A. J. Kellock, J. A. Knapp, and H. J. Whitlow, in *Handbook of Modern Ion Beam Materials Analysis*, edited by J. R. Tesmer and M. Nastasi (Materials Research Society, Pittsburgh, 1995), p. 83.
- ⁴²W. Bohne, J. Röhrich, and G. Röscher, *Nucl. Instrum. Methods Phys. Res. B* **136-138**, 633 (1998).
- ⁴³J. C. Mikkelsen, Jr., *J. Electron. Mater.* **10**, 541 (1981).
- ⁴⁴K. Seeger, *Semiconductor Physics* (Springer, Heidelberg, 2002).
- ⁴⁵R. J. Molnar, T. Lei, and T. D. Moustakas, *Appl. Phys. Lett.* **62**, 72 (1993).
- ⁴⁶D. C. Look, D. C. Reynolds, W. Kim, Ö. Aktas, A. Botchkarev, A. Salvador, and H. Morkoc, *J. Appl. Phys.* **80**, 2960 (1996).
- ⁴⁷J. W. Orton and M. J. Powell, *Rep. Prog. Phys.* **43**, 1263 (1980).
- ⁴⁸B. I. Shklovskii and A. L. Efros, *Electronic Properties of Doped Semiconductors* (Springer-Verlag, Berlin, 1984).
- ⁴⁹G. L. Pearson and J. Bardeen, *Phys. Rev.* **75**, 865 (1949).
- ⁵⁰J. Monecke, W. Siegel, E. Ziegler, and G. Kühnel, *Phys. Status Solidi B* **103**, 269 (1981).
- ⁵¹T. F. Lee and T. C. McGill, *J. Appl. Phys.* **46**, 373 (1975).
- ⁵²B. Podör, *Semicond. Sci. Technol.* **2**, 177 (1987).